A

THESIS

SUBMITTED IN PARTIAL FULFILLMENT OF THE REQUIREMENTS

FOR THE HONORS DEGREE OF

BACHELOR OF SCIENCE IN PHYSICS

Design of a Combined Steering and Focusing Quadrupole

Brock Sayre

DEPARTMENT OF PHYSICS
INDIANA UNIVERSITY

Date 4/28/03

Supervisor: _____
Signature
Typed Name: Vladimir Anferov

Co-signer: _____
Signature
Typed Name: Rick Van Kooten

Design of a Combined Steering and Focusing Quadrupole

Brock N. Sayre

August 10, 2001

Abstract

The energy selection beamline in the Midwest Proton Radiation Institute at the Indiana University Cyclotron Facility is too short to hold all of the steering and focusing magnets that should be placed along it. These serious space constraints have led to a decision to combine the steering function of a dipole magnet with the focusing function of a quadrupole magnet. This would produce a hybrid steering and focusing quadrupole which would take up less space than using the traditional approach of two separate magnets. The steering component of the magnetic field is created inside a quadrupole by transferring some of the current through the coils on one side of the quadrupole over to the coils on the other side. The amount to be shunted over determines the strength of the steering. The control circuitry was designed so that a single steering knob would provide control over the steering without changing the quadrupole's focusing effect.

1 Introduction

Due to space constraints along the energy selection beamline for the Midwest Proton Radiation Institute at the Indiana University Cyclotron Facility, there is physically not enough room for all of the focusing and steering magnets that are normally required to maintain the beam at a level of accuracy and precision appropriate for medical applications. Therefore a decision was made to study the feasibility of modifying a quadrupole to create a hybrid magnetic field inside of it. A dipole magnetic field was to be produced along with the quadrupole magnetic field, creating a single field with a single magnet that adequately performed the functions of both [14].

1.1 The beam requirements for this project

For this project there are several requirements and constraints upon us. First, the steering magnet must be able to, at maximum strength, bend a 205MeV proton beam 5 mrad within the 0.27m of the magnet itself. Second, the quadrupole's magnetic field must not be severely deformed by this process. And third, the steering component of the beam must be easily manipulated in both the positive and negative directions (along the x axis) with the turn of a single dial.

1.2 The Dipole

A dipole magnet is a simple object, with two current-carrying coils wrapped around two poles tips set opposite each other. Figure 1 shows the cross section of a typical dipole magnet.

The magnetic field of a dipole magnet is constant within the gap (see Figure 2). As the magnetic field is constant, the field's effect on a particle's passage through the magnet is independent of position (see Figure 3) , and furthermore can be simply characterized by the Lorentz force law:

$$\mathbf{F_L} = e(\mathbf{v}\times\mathbf{B_{st}}) \tag{1}$$

where here $\mathbf{B_{st}}$ is the magnetic field of the dipole. Note, however, that as the particle's path is bent to the side along the x axis (as it must be with a velocity along the z axis and a magnetic field along the y axis) it is travelling along

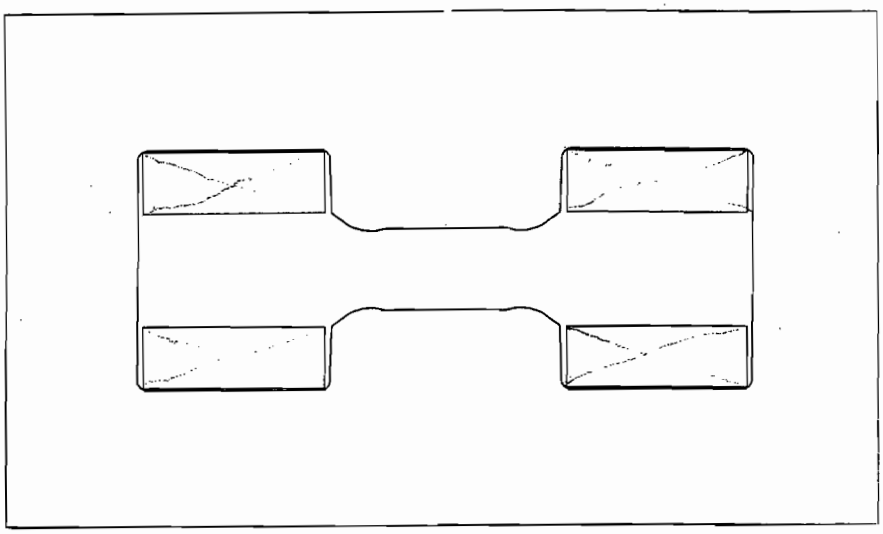

Figure 1: Dipole Cross Section.

a portion of a circle's circumference, and hence must be feeling a centripetal force. This centripetal force is of course just

$$\mathbf{F_C} = m\mathbf{v}^2/R \tag{2}$$

and the particles will travel along a path whereby the forces of Equation (1) and Equation (2) are balanced. Therefore, $\mathbf{F_L} = \mathbf{F_C}$ when a charged particle passes through a constant magnetic field [7].

However, what we are interested in is what the strength of $\mathbf{B_{st}}$ must be to produce the required steering as calculated in the previous section. Therefore, setting $\mathbf{F_L}$ equal to $\mathbf{F_C}$ and solving for $\mathbf{B_{st}}$ yields:

$$B_{st} = mv/eR = \beta p/Le \tag{3}$$

where p is the proton's momentum. For 205MeV protons, which is the maximum energy particles we will be dealing with here, $p = 653.24$ MeV/c. Substituting these values into Equation (3) yields $B_{st} = 0.04035$ T $= 403.5$ G.

1.3 The Quadrupole

The shape and magnetic field of a quadrupole is significantly more complex than that of a dipole, as can easily be seen in Figure 4. While the Lorentz

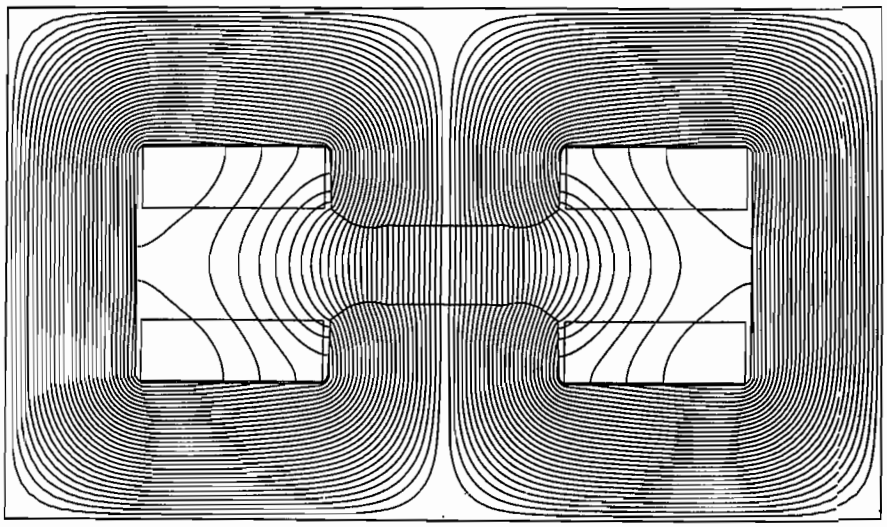

Figure 2: Magnetic Field of Dipole.

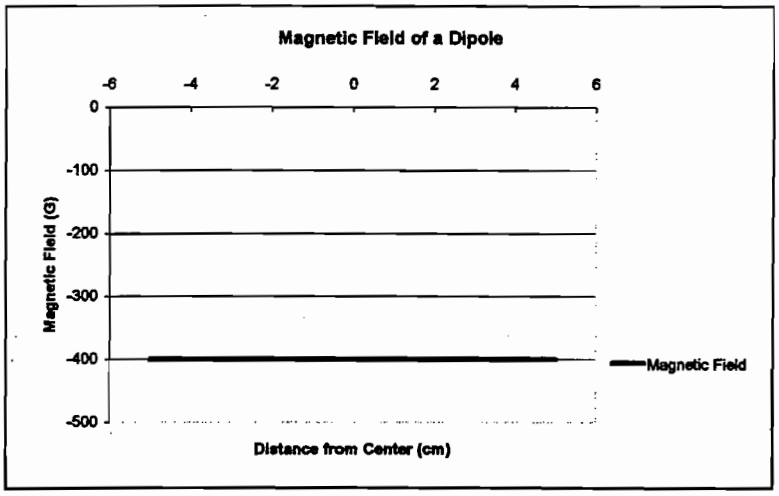

Figure 3: Constant Field of Dipole along X Axis.

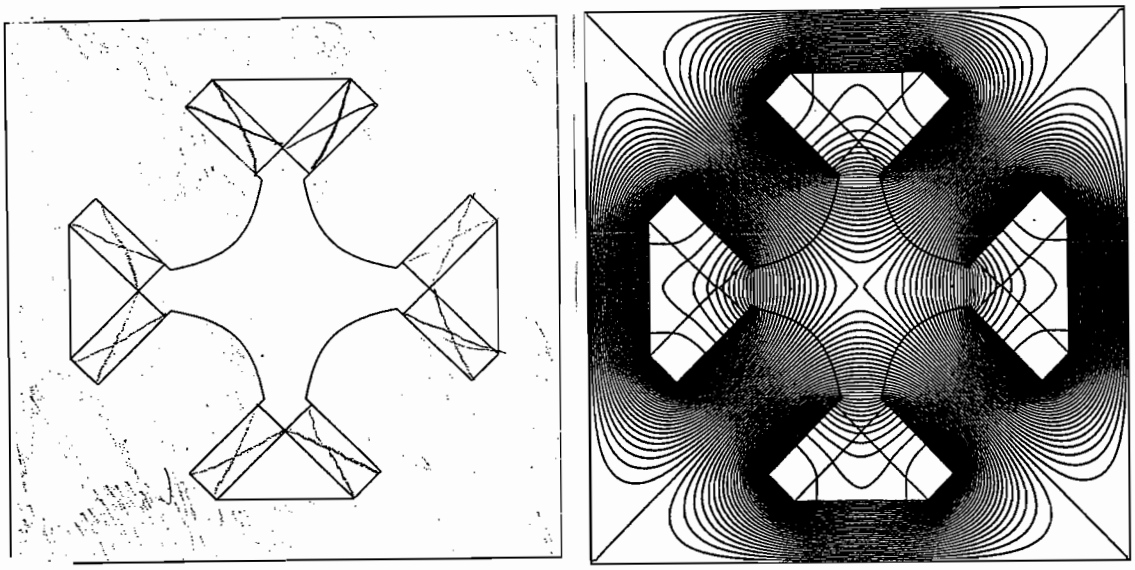

Figure 4: Quadrupole Cross Section and Magnetic Field.

force law still applies to the case of a proton passing through the magnetic field of a quadrupole, the more complicated field of a quadrupole produces a significantly more complex beam deformation than simple bending.

The magnetic field of a quadrupole is most accurately given by the differential equation:

$$\mathbf{B} = \nabla \Phi_m \tag{4}$$

where

$$\Phi_m = B'xy. \tag{5}$$

Of course, Equations (4) and (5) are only applicable to the quadrupole's magnetic field within the current-free air region between the poletips [5, 13]. However, since that is the only region that concerns us (as the beamline and the protons only pass through that region), this is of no consequence.

Further, along the x and y axes, B' can be approximated as

$$B' = 2\mu_0 NI/R^2 \tag{6}$$

so

$$\Phi_m = 2\mu_0 NIxy/R^2 \tag{7}$$

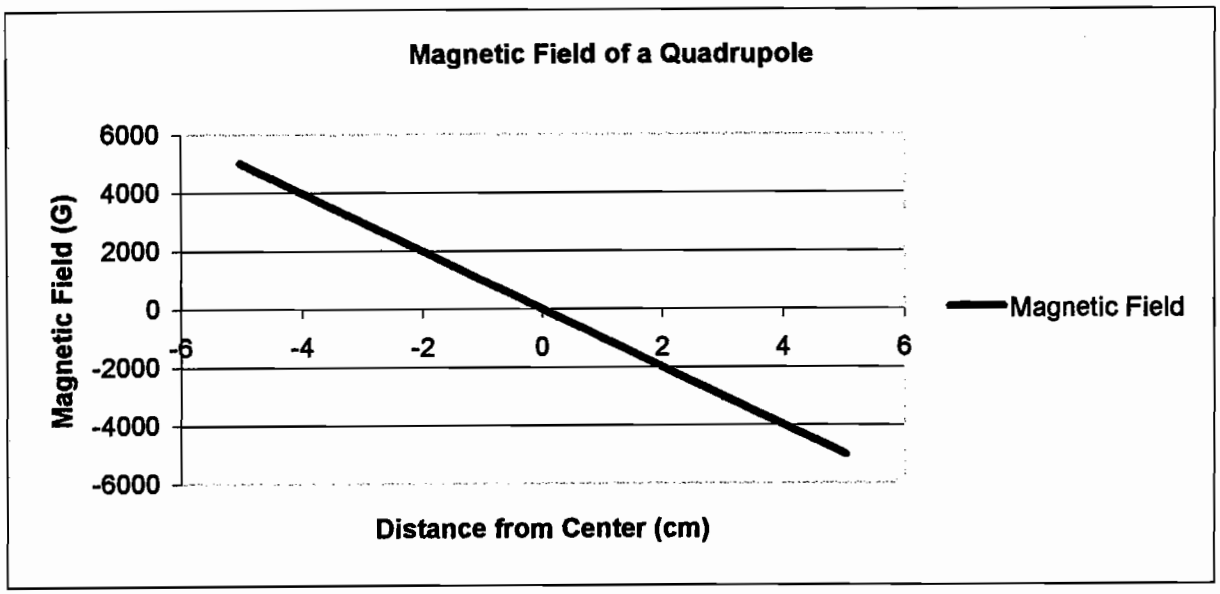

Figure 5: Continuous Linear Field of Quadrupole along X Axis.

and therefore:

$$\mathrm{B} = 2\mu_0 NI/R^2(y, x, 0). \tag{8}$$

Along the x-axis, therefore, the magnitude of the magnetic field of a quadrupole with an aperture radius (R) of 5cm, 53 turns (N), and a current (I) of 200A is:

$$B = 10.66x \text{ Tesla}. \tag{9}$$

But how do protons react when passing through this quadrupole magnetic field?

As a simplification, think only about the behavior of a proton passing through the quadrupole along the x-axis of the quadrupole. Figure 5 has a graph of the magnetic field along the quadrupole's x-axis, of which the most important feature is that while it is no longer constant, as for a dipole magnet, it *is* linear. Further, the magnetic field at the center of the quadrupole is zero. This also all follows directly from Equation (9).

Imagine a proton passing through the quadrupole somewhere along the x-axis. If it passes through the center, it experiences no magnetic field, and hence its trajectory is unperturbed. However, if it is any distance away from the center it does experience a bending force. This bending force has three

characteristics that are important here. The first is that as the velocity of the proton is identical regardless of whether it is travelling along a -x or +x direction, but the magnetic field is opposite in direction, the bending force upon the proton is oppositely directed, depending upon what side of the quadrupole it is on. The second is that because the magnetic field is linear, the magnitude of that bending force is identical regardless of which side of the center the particle is on, for identical displacements from the center.

In short, the two halves of the quadrupole are mirror symmetric about the center. Finally, because the magnetic field is linear, the magnitude increases as you get farther from the center of the quadrupole. The end result is that the quadrupole's magnetic field will either cause all protons along the x-axis to be focused towards the center of the quadrupole or to be defocused away from the center. A close examination of a quadrupole should be enough to convince oneself that if the quadrupole focuses upon the x-axis, then it will defocus along the y-axis, and vice versa. Due to this fact, quadrupoles are often used in particle beams in pairs of magnets with opposite polarity. Due to the laws of optics [15](which apply equally well to magnetic lenses like quadrupoles) the cumulative effect of two quadrupole magnets in the above configuration is an overall focusing of the transverse dimensions of the beam envelope.

2 Superimposing the dipole and quadrupole fields

As we do not have the physical space to put the equipment required to produce a dipole field and then a quadrupole field, we must instead produce *both* magnetic fields in the same place. In a purely mathematical sense, this is simple: merely add together the constant field of the dipole and the linear field of the quadrupole, and then produce the resultant magnetic field in one location. While in practice this becomes more complex, the idea is as simple as that. Examining Figure 6 shows in a quick intuitive fashion exactly what is being discussed. The "Steering Quadrupole" field is merely the result of adding the graphs of the other two fields together.

One can also view the steering quadrupole's magnetic field as being identical to a regular quadrupole of the exact same strength, physically offset

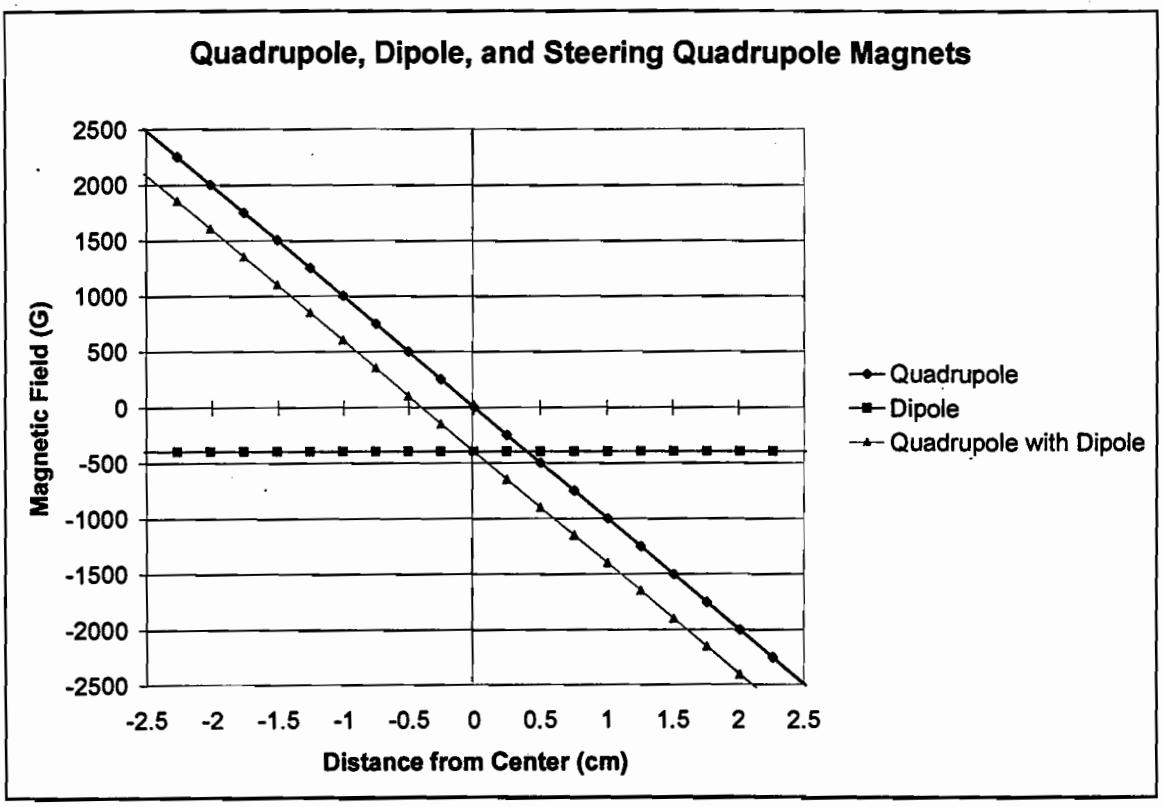

Figure 6: Magnetic Fields of Quadrupole, Dipole, and Steering Quadrupole.

SIDE 1

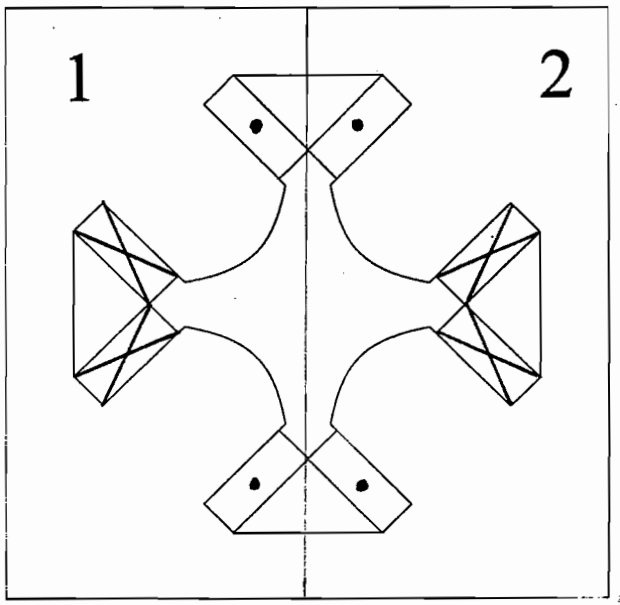

SIDE 2

Figure 7: Structure of Steering Quadrupole.

from the center of the beamline. In this case, all the protons are being bent towards the zero point of the magnetic field, which is no longer at the center of the beam. Hence, while focusing, the beam also produces an overall bending effect towards the new magnetic center of the magnet (which is here no longer the physical center of the quadrupole). The dipole field thus produced is identical to the dipole field that would be required to produce a bending field strong enough to move a proton from the old magnetic center of the quadrupole to the new magnetic center of the quadrupole. Calculating the strength of the dipole thus created will occupy us in the next section.

2.1 Creating a dipole field within a quadrupole

How does one produce this dipole field within a quadrupole magnet? By modifying the amount of current going through the four coils, so that not all four coils are still receiving the same current.

If you look at Figure 7, the quadrupole has been divided into two regions, Side 1 and Side 2. If some amount of current (ΔI) is transferred from Side 1 to Side 2, one ends up with a situation where the two coils on Side 1 are

receiving $2\Delta I$ less than the current being received by the two coils on Side 2. We shall call the modified current running through Side 1 "I_-" and the modified current running through Side 2 "I_+". In the next section it will be determined what $2\Delta I$ is required to produce the needed $\mathbf{B_{st}}$ for this project.

2.2 Calculation of the required current shift

The magnetic field from poletip to center on Side 1 of the quadrupole must of course be modified due to the lower current now running through it. It's new magnetic field can be approximated as:

$$B_1 = 2\mu_0 N I_- / R \tag{10}$$

while on Side 2 the new magnetic field can be approximated as:

$$B_2 = 2\mu_0 N I_+ / R. \tag{11}$$

These equations roughly correspond to the steering quadrupole graph from Figure 6, except that here the magnetic field of the created dipole field is related to the two magnetic fields produced on either side of the steering quadrupole in the following way:

$$B_{st} = (B_1 - B_2)/2. \tag{12}$$

Substituting Equations (10) and (11) into Equation (12) yields the following result:

$$B_{st} = 2\mu_0 N \Delta I / R \tag{13}$$

and solving for ΔI in Equation (13) and substituting the correct values in for N and R and inserting the previously calculated maximum steering strength calculated earlier (403.5 G) produces the final result $\Delta I = 15.17$A, in which case the total difference in current between the two sides of the steering quadrupole is 30.34A.

Therefore, in theory we now know how much current needs to be diverted from one side of a quadrupole to the other to produce the required dipole field as well. A reasonable question would be: to what extent does shunting current from one side of the magnet to the other cause deformations of the field that could impair the focusing properties of the quadrupole? For the answer to this, we turn to the POISSON computer program.

3 POISSON Magnetic Field Simulations

The POISSON computer program was originally produced at the Los Alamos National Laboratories [10], and allows the user to create input files specifying certain variables about an object (dimensions, shape, material, magnetic and electrical properties, amount of current flow, etc.) and the program will use algorithms based upon solving the Poisson equation to completely determine electric or magnetic fields of virtually any object with an impressive degree of accuracy. For this project, only the magnetostatic capabilities of the program were utilized.

3.1 Purpose of simulation

The purpose of performing a series of simulations of a steering quadrupole with POISSON is twofold. One, to determine the amount of field deformation (if any) caused by altering the current distribution through the quadrupole; and two, to determine how accurate the original "back of the envelope" calculations performed in Equations (3) and (10) to (13) in fact were. Some deviations are expected, as multiple approximations and simplifications were utilized in the original calculations, their purpose having been only to determine the original feasibility for this project.

3.2 Problems encountered

POISSON uses symmetry to large degree within its code, partially out of a desire to be as user friendly as possible, but mostly out of a strong desire on the part of the original programmers to use as little memory as possible, a much greater concern when it was originally written ($\approx$1975) than it is today. Therefore, in the case of a simple quadrupole, one need only specify 1/8 of it's entire shape, and POISSON automatically fills the rest in. In the same way, only 1/4 of a dipole need be entered into the input file.

However, due to the way it "fills in" the rest of the shape, 1/4 of a quadrupole *cannot* be entered into it. Sometimes POISSON performs an inversion (changing all positive currents to negative currents and vice versa), and other times it performs a translation (maintaining the direction of the original current). Therefore, my attempt to produce an intermediate step for testing purposes failed, as the current distribution was incorrect when using

1/4 of a quadrupole. I therefore moved directly into the final stage, producing 1/2 of a quadrupole in preparation of altering its current distribution. Luckily, I happened to produce the top half of the quadrupole in my input file, as when it flips the image down to complete the quadrupole it does not invert the currents. If, on the other hand, I had instead created, say, the left half of the quadrupole, the currents would have been inverted when it was flipped, causing it to not behave even remotely like a quadrupole.

Further, when creating the top half of the quadrupole, the desire was for the geometry to be as symmetric as possible. The "ideal" quadrupole has hyperbolic poletips (as the magnetic field lines created within the center follow hyperbolas) and indeed POISSON came with the ability to draw hyperbolas automatically, with the user only providing the two endpoints and the radius. However, as the program expected all quadrupole usage to take advantage of the time-saving nature of the 8-fold symmetry, to save space POISSON did not have to ability to draw a hyperbola anywhere other than the first quadrant. Therefore, for the right half of the quadrupole input file, I instead specified many many points along a hyperbola, and connected them with straight lines.

The initial worry was that this would lead to differences within the program from one side to another. However, as POISSON uses a triangular mesh over which it calculates the Poisson equation, there is a limit to how accurate it is over small regions, and therefore enough points were added along the second poletip so that the "graininess" of the hyperbola was no greater than the "graininess" of the mesh itself, and in fact had to be made less accurate, as POISSON could not handle the level of accuracy originally specified.

3.3 Method of simulation

Figure 8 shows the example quadrupole input file included with the POISSON program. This example was first reduced by the proper factor to reduce the radius to 5cm, and was then extended over the $y = x$ axis to create 1/4 of a quadrupole, then further extended over the y axis to create 1/2 of a quadrupole. The current was then changed to reflect 200A passing through 53 turns of wire per coil. This produced a standard quadrupole, of exactly the dimensions of the quadrupole to be used for this project, as well as prepared the way for the next step. Here has been included the example input

file instead of the final input file because the final version is over 4 times longer, and is no more fundamentally interesting to look at. The "meat" of how POISSON works for quadrupoles is completely contained within the example, and is fairly simple to read. The input file was then run, creating a figure showing the magnetic field lines of the half quadrupole as well as a text file. The text file contains data giving the magnetic field along the x-axis. Using the data from the text file, a graph can be produced. This input file can then be modified so that different current distributions are represented. For this project, a total of seven different current distributions were produced and examined, from the standard quadrupole (0A difference), to a high degree of steering (with a 60A difference in current from Side 1 to Side 2). The results are given in the next section.

3.4 Results of simulation

Here are displayed both the POISSON-created images and the resulting graphs based off of the data from the POISSON-created text file. Note that visually there is almost no apparent difference between the 0A (standard quadrupole) and even the 60A (out of 200 amps, remember) cases. This is positive, as the major concern (and much of the reason for running the POISSON simulations) was that shunting current from one side to another could result in a gross deformation of the field, introducing large non-linearities which would virtually destroy the focusing capabilities of the quadrupole and introduce significant higher order multi-pole moments. At an initial viewing, such does not seem to be the case:

In Figure 12, the graphs of all seven calculated configurations are represented, once again showing how little the field has been distorted, as the lines are virtually on top of each other. There is a small amount of distortion apparent on this graph, as the higher current differences are beginning to "sag" a little bit at the ends. However, examining the closeup graph shows that within a centimeter of the quadrupole's center, the different fields are quite linear even still (which is where most of the beam will be) and that increasing $2\Delta I$ does indeed cause the magnetic center of the quadrupole to shift along the x axis, just as predicted. In the next section, the data will be analyzed to a more precise degree.

QUAD

```
 1  quad with hyperbolic curve, input table 9/12/86
 2  $reg nreg=4,dx=0.35,dy=0.35,xmax=33.5,ymax=33.5,
 3       npoint=5$
 4  $po x= 0.000, y= 0.000 $
 5  $po x=17.444, y= 0.000 $
 6  $po x=33.080, y= 0.000 $
 7  $po x=33.080, y=33.080 $
 8  $po x= 0.000, y= 0.000 $
 9  $reg mat=3, npoint=9$
10  $po x= 5.837, y= 5.837 $
11  $po nt=3, x=13.507, y= 2.523, r=8.255$
12  $po x=14.214, y= 3.230 $
13  $po x=22.470, y=11.486 $
14  $po x=25.700, y= 8.256 $
15  $po x=25.700, y= 0.000 $
16  $po x=33.080, y= 0.000 $
17  $po x=33.080, y=33.080 $
18  $po x= 5.837, y= 5.837 $
19  $reg mat=1, cur=11416.4, npoint=5$
20  $po x=14.214, y= 3.230 $
21  $po x=17.444, y= 0.000, new=-1$
22  $po x=25.700, y= 8.256 $
23  $po x=22.470, y=11.486 $
24  $po x=14.214, y= 3.230 $
25  $reg npoint=2, ibound=0$
26  $po x= 0.000, y= 0.000 $
27  $po x=33.080, y=33.080 $
```

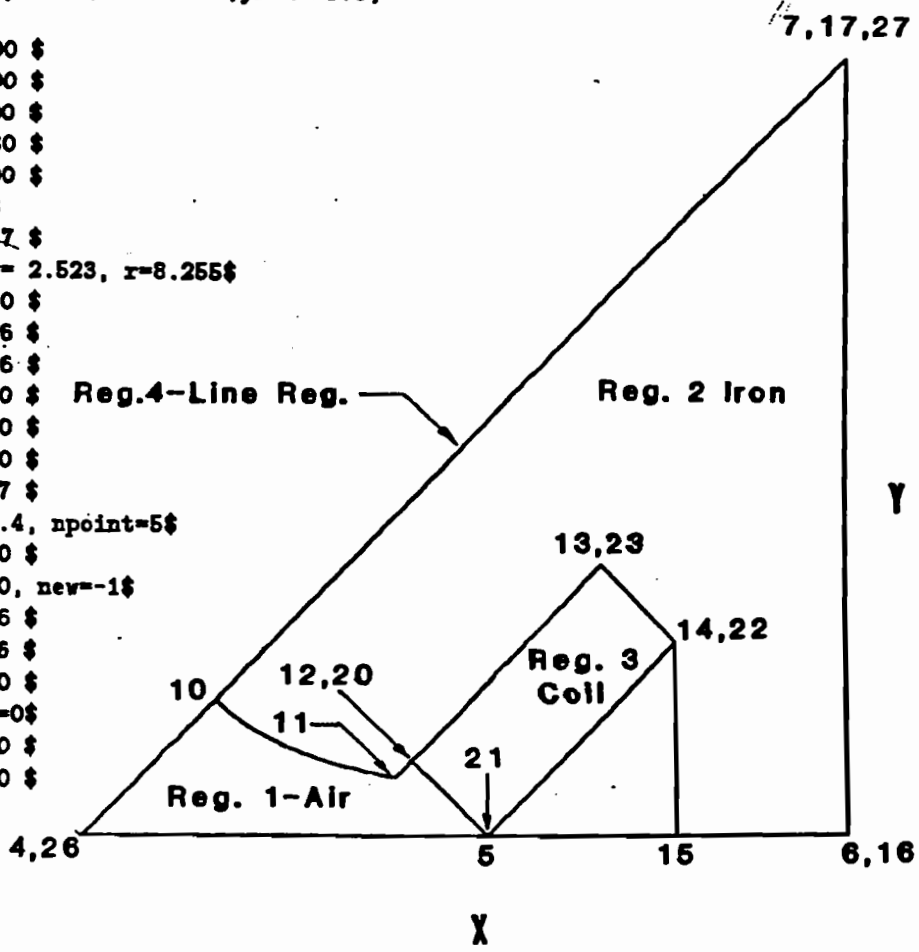

Figure 8: Program fragment for POISSON.

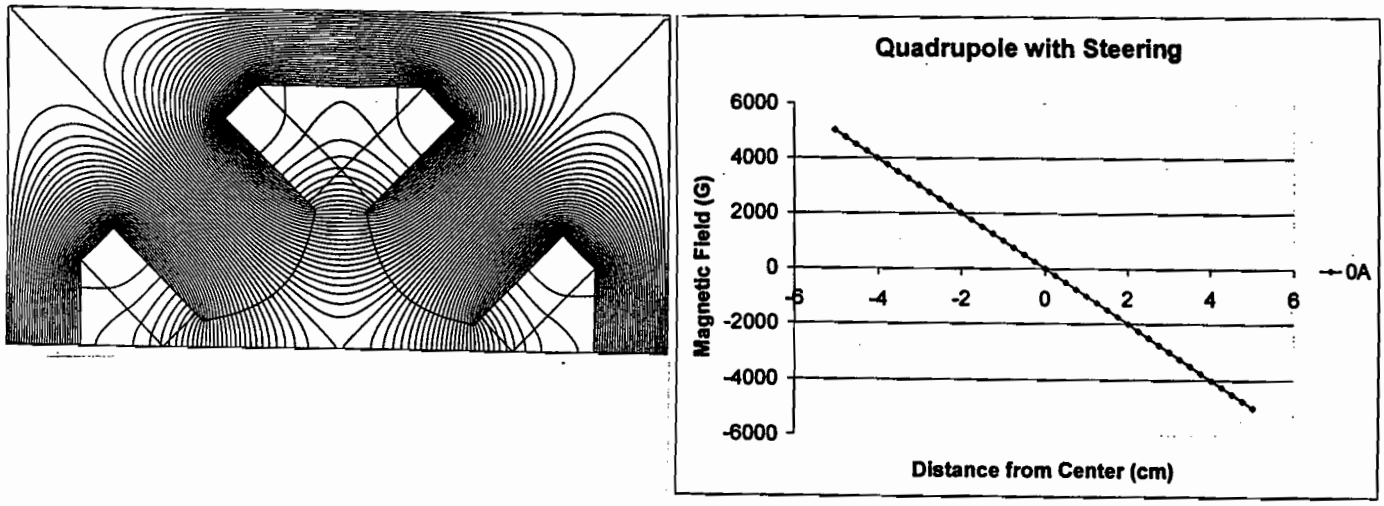

Figure 9: (0A Steering Quadrupole, image and graph.

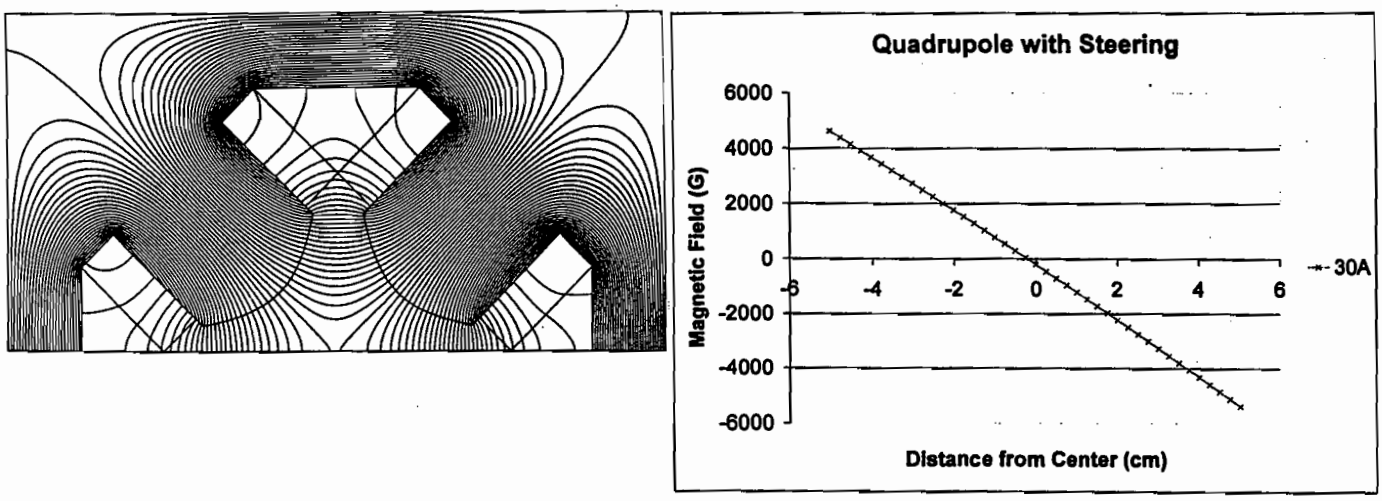

Figure 10: 30A Steering Quadrupole, image and graph.

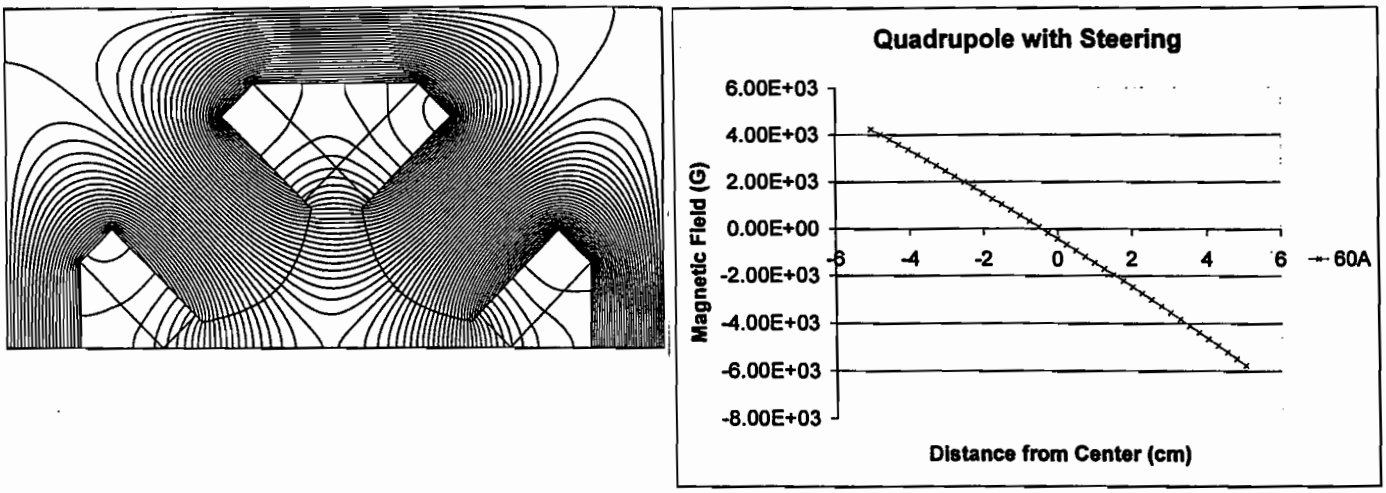

Figure 11: 60A Steering Quadrupole, image and graph.

3.5 Data analysis

Since the entire theory of how and why we can create dipole fields within a quadrupole by adjusting the current distribution within it's coils relies upon the fact that the final steering quadrupole's magnetic field will be a mathematical superposition of a standard quadrupole's and a dipole's magnetic fields, the obvious method to determine whether or not the required dipole field has been produced is to subtract the 0A case (the non-steering quadrupole) from the steering cases (10A to 60A) and plot the resulting data. If all goes well, it should produce a series of lines of constant value, with the 30A case close to the 400 G point. In Figure 13 we have done precisely that, and see that according to the POISSON simulations, the resulting field is at least to a first approximation a constant dipole field. Further, we see that the field *is* approximately constant near the center of the beamline. This is desirable, as the steering quadrupole will only be used to make small steering corrections to the beam (5mrad) to tap the beam back into an optimal position. Therefore, if the beam is significantly further askew than 1 or 2 centimeters, then steering magnets much further upstream need to be more accurately aligned. The purpose of this magnet is not to have major steering power, or indeed even to steer it regularly, but instead to merely set it to a certain steering value to correct for a minor asymmetry from upstream and leave it there.

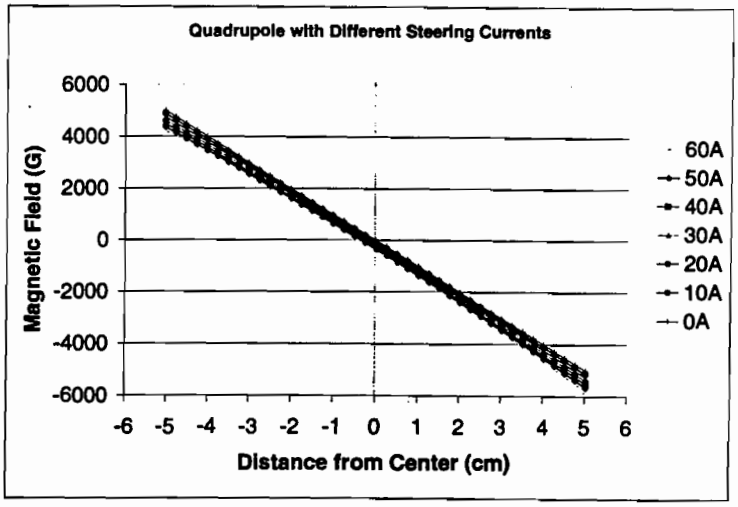

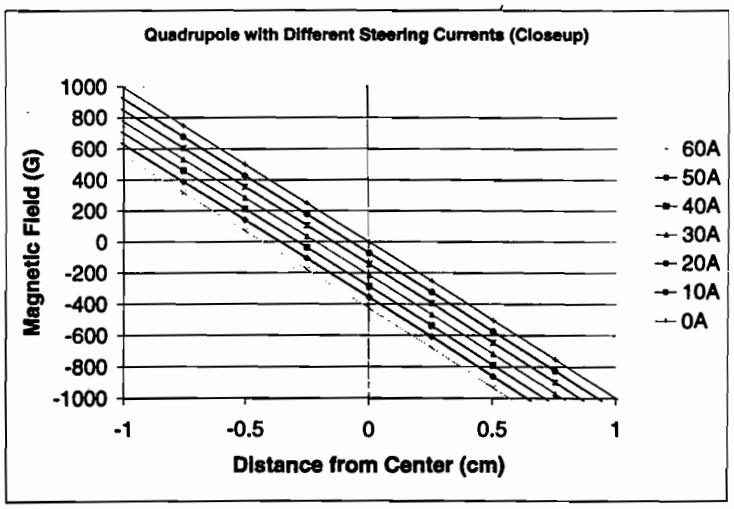

Figure 12: Multiple Steering Quadrupoles, and Closeup of Same.

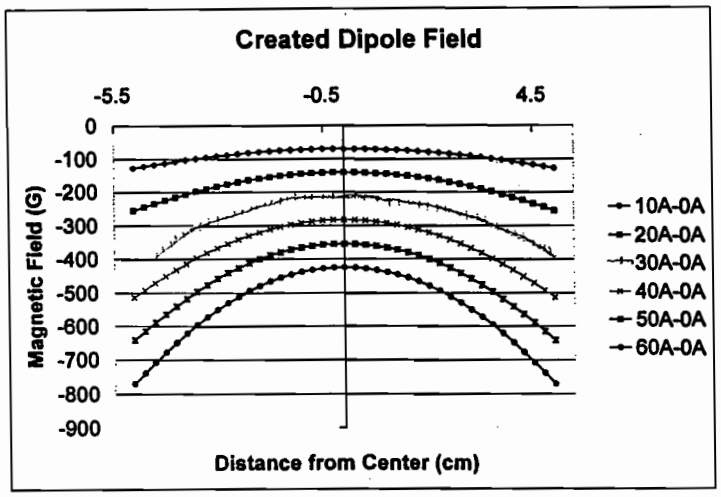

Figure 13: Dipole Field Strength Due to Current Asymmetry.

Also from Figure 13 the $2\Delta I$ required to reach 400G looks to be approximately 55A, as opposed to the 30A derived from Equation (13) earlier in the paper. This difference is due to several factors, but chief among them is a subtlety ignored previously when calculating the expected 30A. When performing those calculations, the shifting of the magnetic center of the quadrupole was glossed over, but in actuality there is a $\sqrt{2}$ that should have been multiplied by the 30A due to the superposition of *two* magnetic centers (one produced by each pair of North-South poles). Also, as the assumption of linearity was so strong in the initial calculations, it is in fact more proper to compare the initial 30A to the *average* magnetic field of the POISSON-created dipole fields from Figure 13. Utilizing both of these correction factors, the 30A is transformed to approximately 42.9A, and if one also takes the average value of the 40A-0A POISSON values, one gets an average dipole magnetic field of approximately 365G, which places our hand calculations and our POISSON calculations on much closer ground to each other.

However, for the purposes of designing and running an actual steering quadrupole, the numbers from POISSON are far more trustworthy than the original calculation, whose sole purpose was to get us within an order of 2 or so of the correct current distribution.

As for additional analysis of the created dipole fields, the next logical

step would be to subtract a constant term from them and take the resulting field and determine *its* strength. Even a casual glance will assure one that it is a sextupole magnetic field. In this case, according to POISSON, we have the correct quadrupole field overlaid with the correct dipole field, and a small sextupole perturbation to the field. Calculating the effect of that sextupole field upon the proton beam would essentially finish all analysis of how we can expect a proton beam to behave after passing through our steering quadrupole. A rough estimate of the strength of the sextupole field at maximum steering at about 2cm off center shows that the sextupole has a magnetic field strength here of about 37 G, whereas the quadrupole's field strength is 2132 G and the dipole's field strength is 284 G. Therefore, the sextupole strength even at maximum distortion (for high steering, beam relatively near center) is only about 10% of the the dipole field strength and 2% of the quadrupole's field strength.

A question not answered here is whether or not the induced sextupole enhances or hinders the quadrupole, as sextupoles are often used to correct for dispersion problems with quadrupoles. If the energy selection beamline has a sextupole already in it, it may be possible to adjust it's strength to partially cancel out the effect of this induced sextupole moment, which certainly bears consideration. Of course, there are undoubtedly even higher multi-pole moments as well, but should easily fall well beneath the 1% perturbation mark.

4 Construction of Instrumentation

A series of calculations were initially performed to determine a method of creating dipole and quadrupole fields of the appropriate strength in the same region. Then, having calculated that an imminently possible current distribution is required, POISSON simulations were run to verify and firm up the initial predictions. This leads directly to the next phase of the project: to begin building.

The actual physical process of shunting more than 15A from one side of the quadrupole to the other is relatively complex, the control mechanisms associated with this are even more so, and the overall design requires many parts. While in a later section much of the details of the control mechanisms and shunting process will be described, for now the focus is upon a few pieces of vital equipment that were constructed as a preliminary to the main thrust

of the hands-on portion of this project.

For now, it is important to realize that objects called "passbanks" will be the physical objects shunting the current from Side 1 of the steering quadrupole to Side 2, and further, as they will be carrying more than 30A of current at times, they have to be adequately protected from dangerous fluctuations in current.

4.1 Universal AC interlock for small DC supplies

While designed and built for this project, the "Universal AC Interlock for Small DC Supplies" is, as the name suggests, useful in a myriad of circumstances. The important concept to understand throughout this section and throughout the rest of this paper, is that whenever possible one would like to control large currents through the clever control of small voltages. The reasons for this are clear. For safety reasons, one hesitates to have controllers and operators having to regularly work right next to large current sources. For this reason the conceptually cleaner design of merely having a large potentiometer running from one side of the quadrupole to the other, with the potentiometer sitting in the control room, is a very dangerous and energy inefficient method. Additionally, small voltages are very easy to control and manipulate with thousands of small, off-the-shelf bits of digital electronics, while objects to handle large currents tend to be bulky, expensive, and little given to complex logic structures. The Universal interlock steps right into that breach, literally, by allowing this to happen. The interlock has it's own need for power (a basic wall outlet will do), and puts out a small DC voltage from its side. Then, instead of plugging large AC power supplies that draw a great deal of current directly into the wall, they plug into the interlock. The interlock then has additional plugs that run into the wall for your heavy current (20A to 30A) 120V and 240V wall current. The small DC voltage is then set up as part of a system, any system will do, whereby the circuit is normally closed, allowing that small voltage to pass. This small voltage operates a contactor, which is no more than a coil of wire with a spring-loaded conductor running inside of it. When the small DC current runs, the coil is energized, creating a tiny magnetic field, and attracting the conductor. The conductor is held down, completing the circuit between the heavy load power supplies, and the large wall currents. As soon as the small DC circuit is broken, however, the spring-loaded conductor is released, breaking the large AC

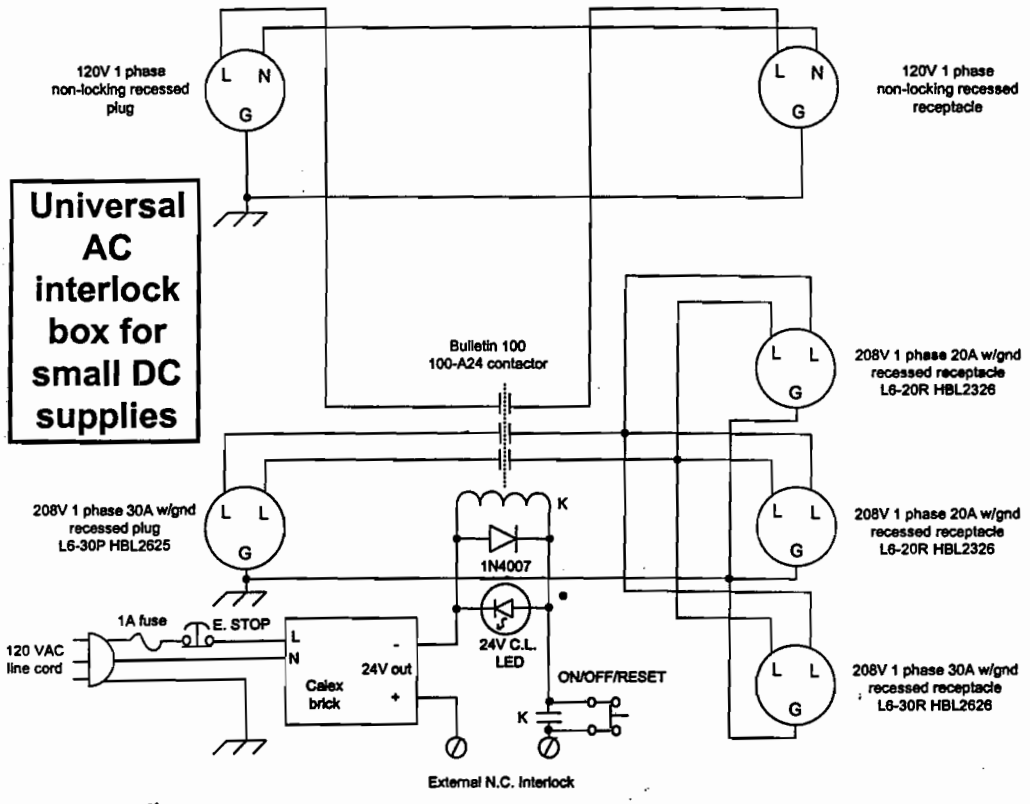

Figure 14: Schematic of Universal AC Interlock [4]

high-current circuits immediately.

The beauty of such a system is that it allows for large AC power supplies or currents to be remotely turned on and off by manipulating a small current DC voltage. Further, this DC circuit can be as complicated as you desire. For our purposes, there is a manual turn-off on the box which cuts the DC, as well as a flow switch [12], constantly monitoring the flow of coolant water to the passbanks (more on that later), and a connection to a second box, which monitors the fuses. All of these connections are, of course, in series with each other, so that any one break in the circuit breaks the entire DC circuit.

4.2 Fuse trip interlock box

The fuse trip interlock box has a very similar (though more specific) function as the universal interlock above. Each passbank contains 14 fuses to protect it's circuitry (to follow shortly). These fuses are known as pop-up fuses or identifying fuses, in that when they blow, they fire a small pin several centimeters out of one end. The fuse block itself is set up in such a way so that if a single fuse blows, it's pin makes contact with a small metal bar. This completes a small current DC circuit from the fuse trip interlock box through the trip bus (where the fuse hits) through the end of the now defunct fuse, through the power lead supplying the main current to the passbank, and back to the fuse trip interlock box. This completed circuit sends a signal through the box, which throws a small switch. This switch is attached in series to the DC circuit of the Universal interlock, therefore shutting off the power to the passbanks. This means that even a *single* blown fuse immediately cuts all power to the entire quadrupole. Two passbanks per quadrupole and 14 fuses per passbank mean 28 fuses being watched intently at all times, any one of which blowing immediately shuts down the circuit.

4.3 Other equipment

While working on this project, several other small items were built to perform other subsidiary tasks, such as two power cords to run the high current from the Universal interlock to the power supplies, and a line cord running a third power supply to a wall current. In addition, piping for water coolant systems, and other such miscellany were built or assembled.

5 Passbank Design and Construction

Now the detailed structure of the passbanks and how they function will be discussed.

5.1 Basic concept

The concept of the passbank is merely to have some mechanism whereby some amount of current can be diverted from one side of the quadrupole and added to the current being received by the other side of the quadrupole. This symmetric method of current addition and subtraction was settled upon as it easily enables for it to be controlled with a single knob. In Figure 16, the passbank is viewed as a "black box", merely an as-yet-unidentified object that allows some variable amount of current to pass through it and no more. Regardless, the basic idea is quite easy to follow, and shows how the current through both halves of the quadrupole can be varied and indeed can be increased to either side.

Figure 17 shows the actual structure of the passbank. In the figure the passbank is attached to a master-slave power supply system instead of to a quadrupole (for testing purposes, to be discussed in more detail later) but the premise is identical. Here the passbank consists of a MOSFET transistor in series with a 4Ω resistor (the actual passbank has 14 of these in parallel with each other). The Gate Drive Supply uses a small DC voltage to control the MOSFET, allowing a variable amount of current to pass through it [9]. Once again, a small voltage supply is being manipulated to control a large current supply. The fuses in the figure are the fuses mentioned earlier in reference to the fuse trip interlock box.

The small voltage applied to the MOSFET adjusts the amount of current the MOSFET will allow to pass through it, making them very useful for this application.

5.2 Limiting factors

There are several limiting factors associated with these passbanks. First, the MOSFETs themselves have a maximum current load they can withstand, which in the case of the MOSFETs used in this project (IRFP260N) is 35A. Second, the resistors themselves are only rated to handle 25 Watts. Third,

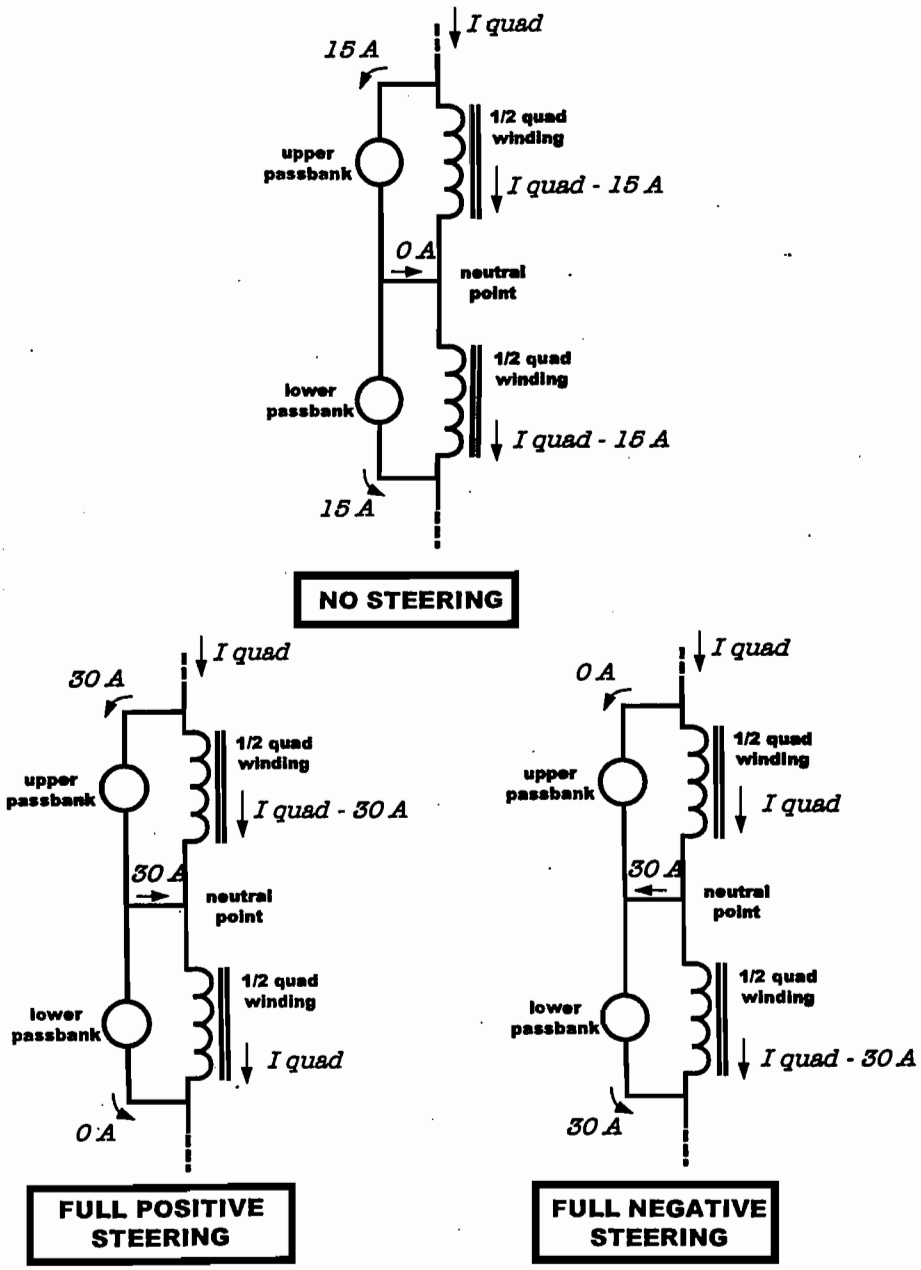

Figure 16: Passbank Concept Diagram [2].

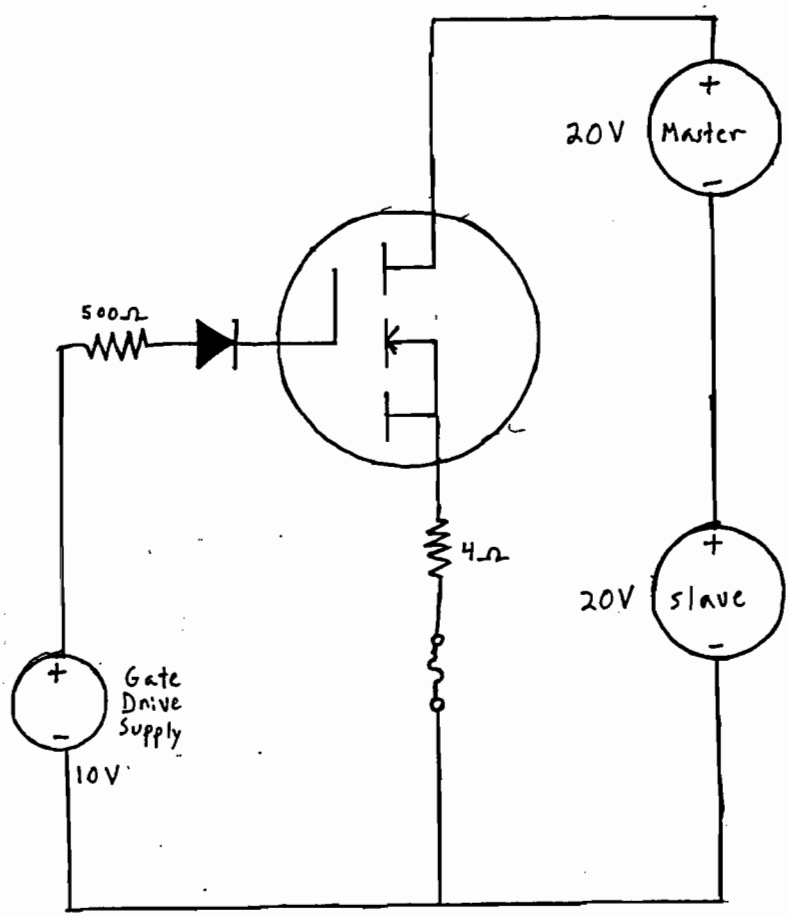

Figure 17: Simplified Passbank Schematic

the MOSFETs have a maximum temperature rating of 175^o C. Fourth, the MOSFETs have a maximum voltage rating of 200V. Note, however, that 40V is the voltage at which the quadrupole is ran, so this is hardly a concern. As each MOSFET can handle 300 Watts just by themselves, the limiting factor is very much either the power dissipation of the resistors, or the temperature of the MOSFET junction. Tests that were performed to study these factors will be addressed in greater detail later.

The detailed reasons for why these particular MOSFETs were chosen, and more complete analysis of their limitations can be found in reference [3].

5.3 Final design

The final design of the passbank system calls for a logic structure and control structure as seen in Figure 18. This will be fleshed out in more detail once we get to the design of the PC board, but for now we turn to testing the final passbanks.

6 Passbank Burn-in Reliability Tests

The passbanks, once designed and built, had to be tested before they were implemented to be sure that they would be able to endure the rigors of high-current usage indefinitely.

6.1 Purpose of test

The purpose of this test is simply to give the passbanks a chance to fail under controlled circumstances, and observe what, if anything, is wrong with their design or construction. MOSFETs have a tendency to allow more current to pass through them as their temperature increases, but of course as more current passes through them their temperature tends to increase. The possibility for an ugly feedback loop is apparent. The fundamental question to be answered is: Are 14 MOSFET transistors and their resistors in parallel stable over time? That is, will the current continue to be shared equally among the 14 transistors, or will one of them begin absorbing more and more of it? If that happens, the fuses of course should save the transistor, and in the

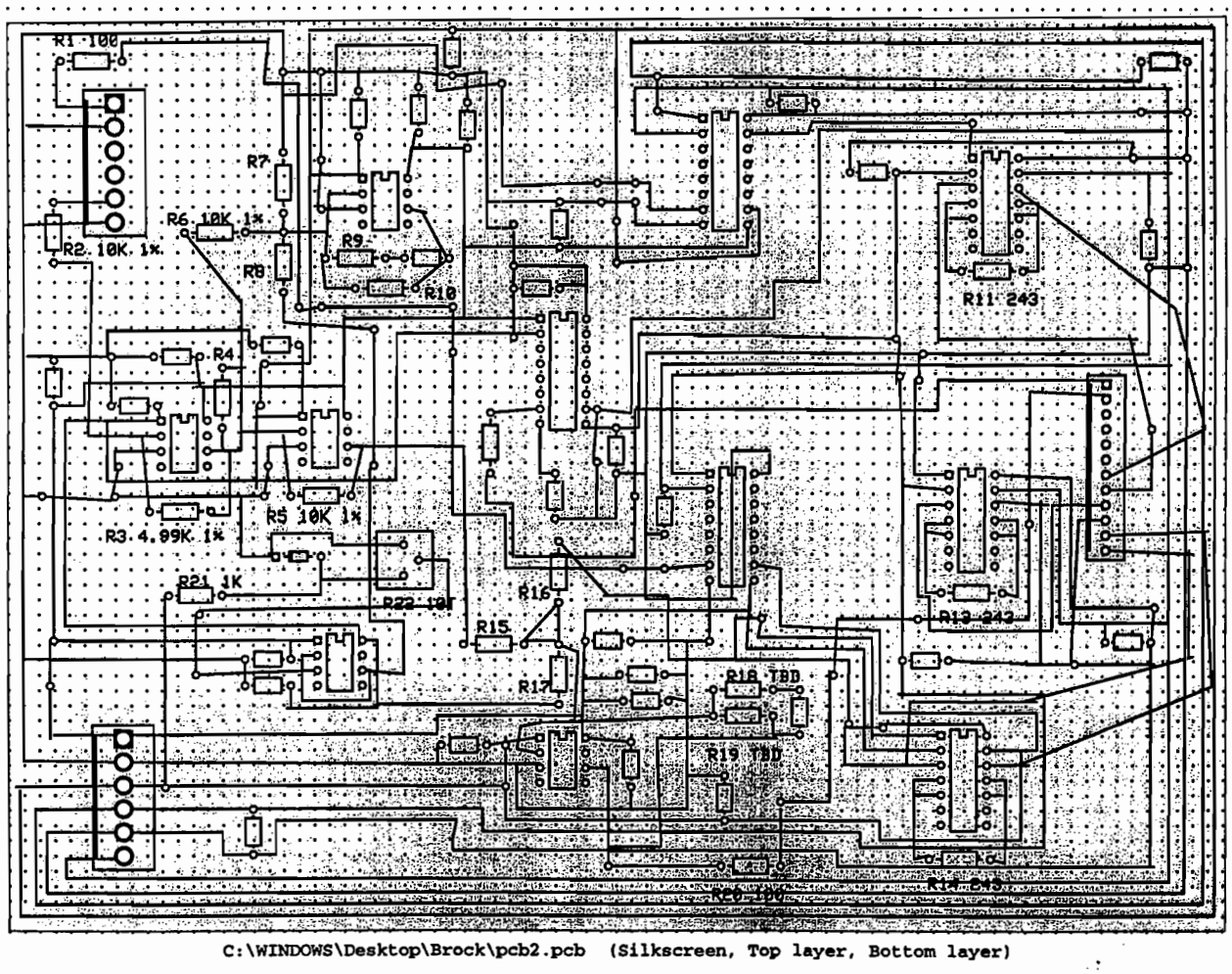

Figure 22: Actual layout of PC Board.

8 Conclusions

Due to space constraints, we resolved to determine whether or not it would be practical to combine two magnets functions into one magnet, how to accomplish that goal, and then finally to build and test the resulting hybrid magnet.

After 10 weeks of work, several of the project goals have been accomplished. First, the initial calculations suggested that indeed a quadrupole could be modified by shunting current from one side to the other to create a dipole field along with the quadrupole field within the newly modified quadrupole. Second, computer simulations using POISSON showed that our initial calculations were close, and that the magnetic deformations caused by this approach were predominently a sextupole moment, with a relative strength of less than 10%, for almost all uses of the steering magnet. Third, we successfully designed and built all the equipment required for this project. This includes not only the passbanks themselves, but also the PC board to control the passbank system, and several interlock systems to protect and further control the entire steering quadrupole assembly. Finally, we rigorously tested the passbanks, looking for signs of instability or inaccuracy. The passbanks performed admirably, passing every test with flying colors, never getting above 68% of the maximum rated temperature, and with current fluctuations within individual MOSFET transistors of less than 1%. Further, all the interlock and safety equipment performed without a hitch, shutting down the entire system before a single component could be damaged over the entire 140 hours of passbank run, excepting a few fuses blown due to initial faulty power supplies, which caused the entire system to shut down just as it should.

A few further analyses of the data could be run in the future. First, the exact strength of the sextupole moment could be calculated, and then compared to known sextupole behavior to predict its effect upon the proton beam. Second, a more exact determination of the maximum current the passbanks can carry could be determined through the rough method of increasing the current until they overload, and observing what effect that has.

In the future, several tests remain to be run. First, the completed quadrupole assembly must be magnetically tested, probably with a hall probe and magnetic field mapper, once again under different configurations, to compare to the simulated results from POISSON. After that the steering

the MOSFETs is 20V, and the project never took it above 10V.

6.3 Taking the data

After the drive gate power supply is adjusted until the proper current is read off of the shunt (20A for passbank 1, 30A for passbank 2) the reading can be taken. At this point the passbank is left on for an extended period of time, with measurements taken only a couple of times per day. The measurements are voltage measurements taken across the 4Ω resistor. As the current through the resistor is the same as the current through the transistor, and the voltage drop across the resistor is proportional to the current (through Ohm's law), then by measuring the voltage drop across the resistor the current through the transistor can be easily found.

The data was taken over an extended period of time, over sixty hours of run time was logged for each passbank. The water pressure in the cooling system was set to 44PSI. In addition to measuring the voltage drop across each of the 14 resistors multiple times daily until the total hours had been reached, multiple temperature readings were taken as well, directly over the MOSFET.

6.4 Analyzing the data

After finishing the data collection, graphs were made directly from the raw data, here shown in Figure 20. Passbank 1 was ran at 20A, and passbank 2 was ran at 30A. There was almost no variation over time in the current draw of any of the transistors over the testing period. In each case, the measured voltage across the resistor should not get above 10V, as at that point more than 2.5A would be passing through the transistor, which would blow the 2.5A fuse, though wouldn't cause any other damage. Note that during the burn-in for Passbank 1, resistor 6 gave an usually high reading for much of the middle portion of the graph. This reading is completely spurious. What occurred was that the fuse on MOSFET 6 had blown, but due to a slight wiring problem (since corrected) the fuse trip interlock box had not properly done its job and shut off the power. The unusually high reading was caused by a slight feedback loop giving the appearance of current going through the resistor. More interesting, however, is the fact that over that period where fuse 6 was blown, the additional current was simply equally divided among

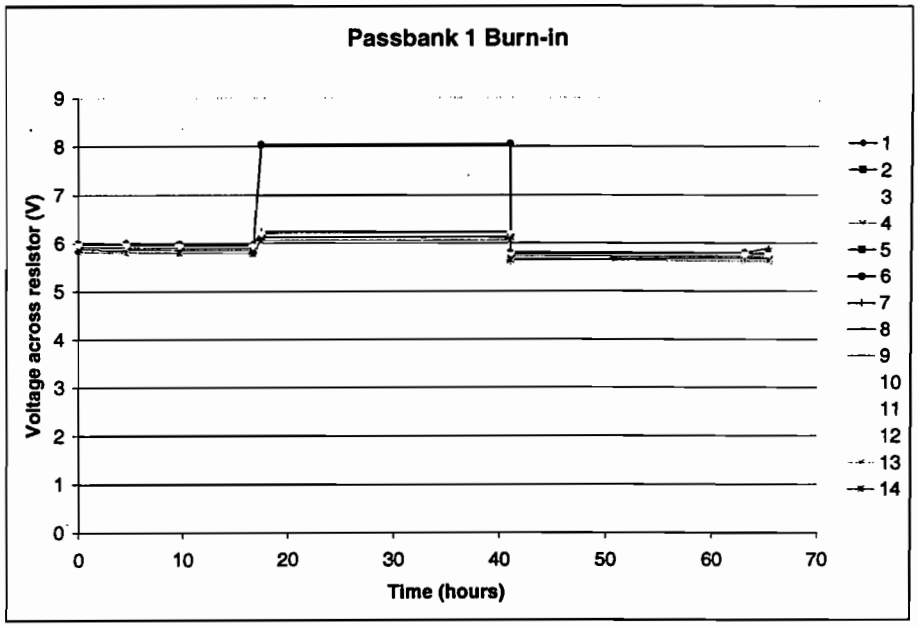

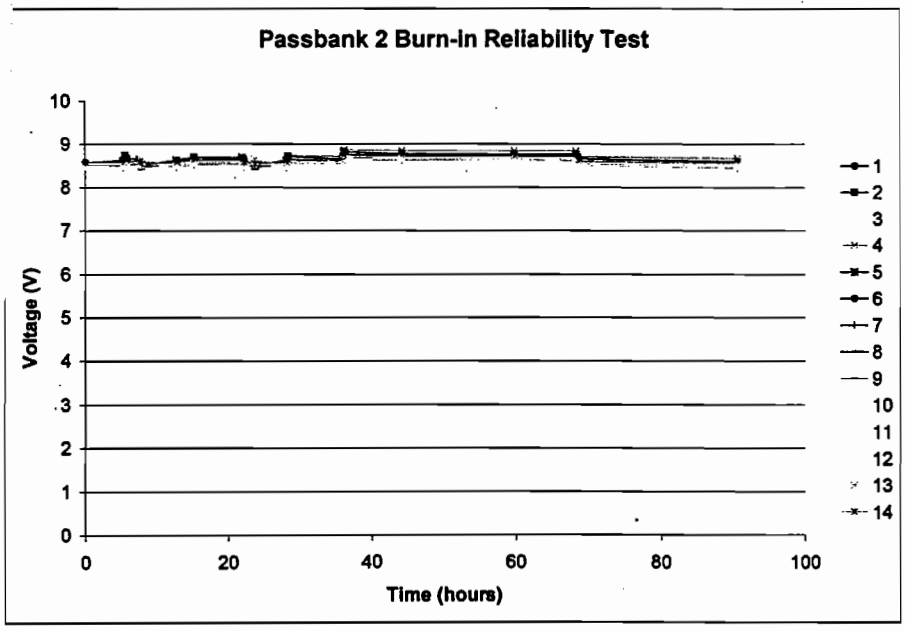

Figure 20: Results of Burn-In for Passbank 1 and 2.

the remaining 13 MOSFETs, causing them all to go up slightly, but not affecting the stability of the passbank at all.

Passbank 2 had no similar problems, as the wiring error had long since been fixed, and as a result, even when the passbank was being ran at its highest rated setting (30A) the entire passbank remained very stable, and under the 10V danger line. While Passbank 2 did show a stronger tendency for the relative amount of current to shift among MOSFETs than did passbank 1, the effect is still quite small, less than 1%.

The final issue to be discussed in analyzing the passbank data is the temperature. Temperatures were collected heavily throughout the runs, from various places over the copper body of the passbank. In this case, only the highest reading matters. The highest temperature, 56° C, was recorded about halfway through the run on passbank 2. This number can be inserted into the following equation to determine the temperature of the actual junction itself within the body of the MOSFET, which after all is the place where the temperature matters most.

$$T_J = T_S + AV(R_{\Theta JC} + R_{\Theta CS}) \tag{14}$$

Here A is the current through the MOSFET, which for passbank 2 is just 30A/14, or 2.14A, while V=40V, $T_S = 56°$C (the temperature of the sink the MOSFET is mounted to). $R_{\Theta JC}$ is the thermal resistance from the junction to the case of the MOSFET, while $R_{\Theta CS}$ is the thermal resistance from the case of the MOSFET to the sink (assuming thermal grease was used, which was). Substituting the appropriate values into Equation (14) (most of which come directly off of the data sheet[11] for the MOSFET) yields:

$$T_J = 56 + (2.14)(40)(0.5 + 0.24) = 119.43° \text{ C} \tag{15}$$

And obviously 119 is less than 175, which is the maximum rated temperature the MOSFET can operate at within parameters.

Therefore, from analyzing the data taken during burn-in reliability runs on both passbanks, we can see that in fact the passbanks are very stable, and never come dangerously near their tolerances at any point, even when ran near the edges of what they were designed for, leaving a generous margin of error.

7 Control of the steering quadrupole

Now that the passbanks have been designed and tested, it now only remains to design and construct the control mechanisms for the passbanks.

7.1 Basic concept

The essential premises are two-fold in the design of the passbank control system. First, a small voltage source that controls the large currents running through the passbanks would enable greater control and safety; and second, the user of the steering component of the magnet should only have to adjust one knob, turning it either clockwise or counterclockwise (depending upon which direction they wish to turn the beam) in the exact same way as they would manipulate a standard dipole steering magnet.

7.2 Final design

The final design calls for a PC board to be attached to the passbanks, to automatically give both passbanks the proper voltage, which causes them to allow through the correct current. Also, the PC board will constantly monitor and modify the current running through the passbanks, and to allow the control knob to simply "tell" the PC board how much voltage to supply to each passbank. In Figure 21 is the final design for the PC board, and it is shown in context with all of the other basic equipment.

7.3 PC board layout

Having been assigned to transform the PC board schematic into an actual PC board, I downloaded a program from a company called "ExpressPCB" from their website [6] and used it to lay all of the components out and create a final design for the board, which can be seen in Figure 22.

This layout was then emailed to the company, who quickly created the board and mailed it back for us to attach the components and finally be able to assemble the completed steering quadrupole: the passbanks, the control systems, the subsidiary equipment, and of course the quadrupole.

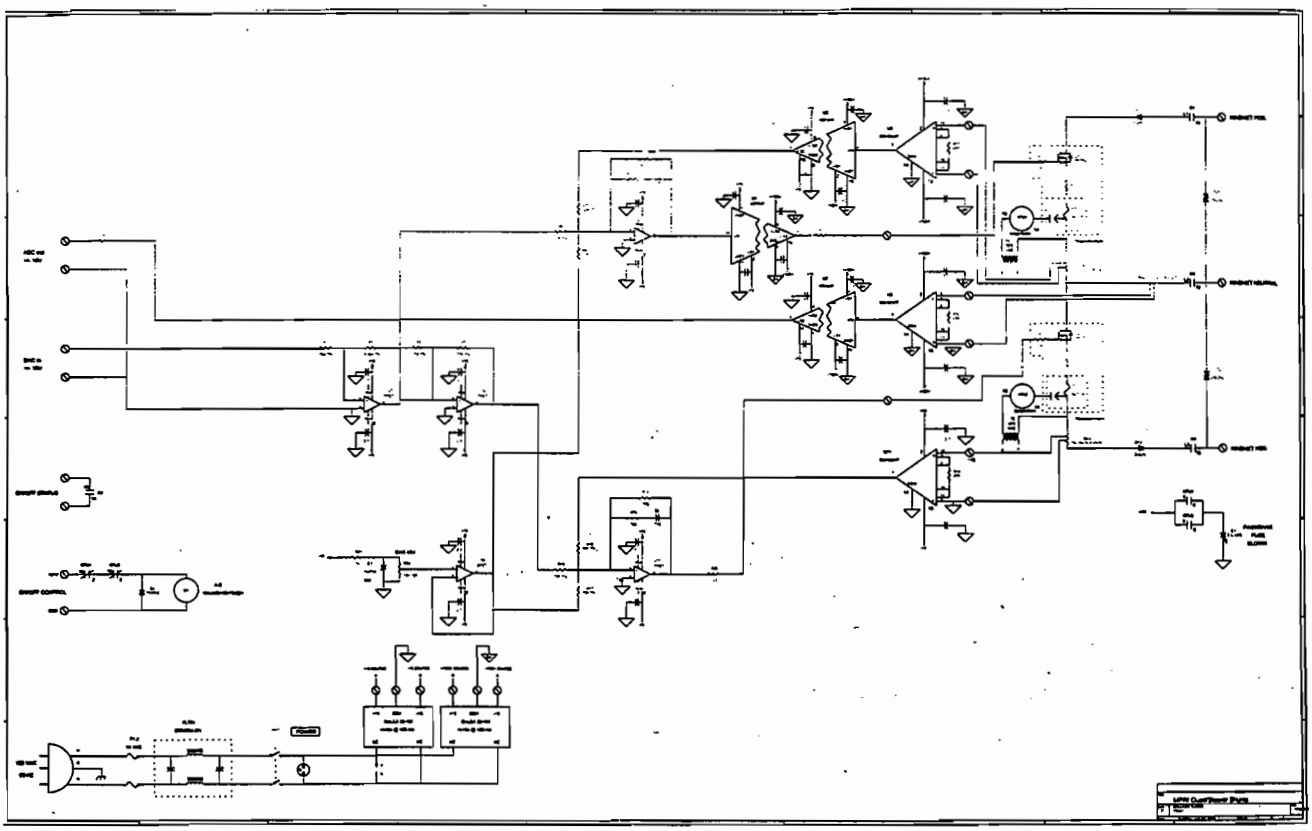

Figure 21: Final PC Board Design.

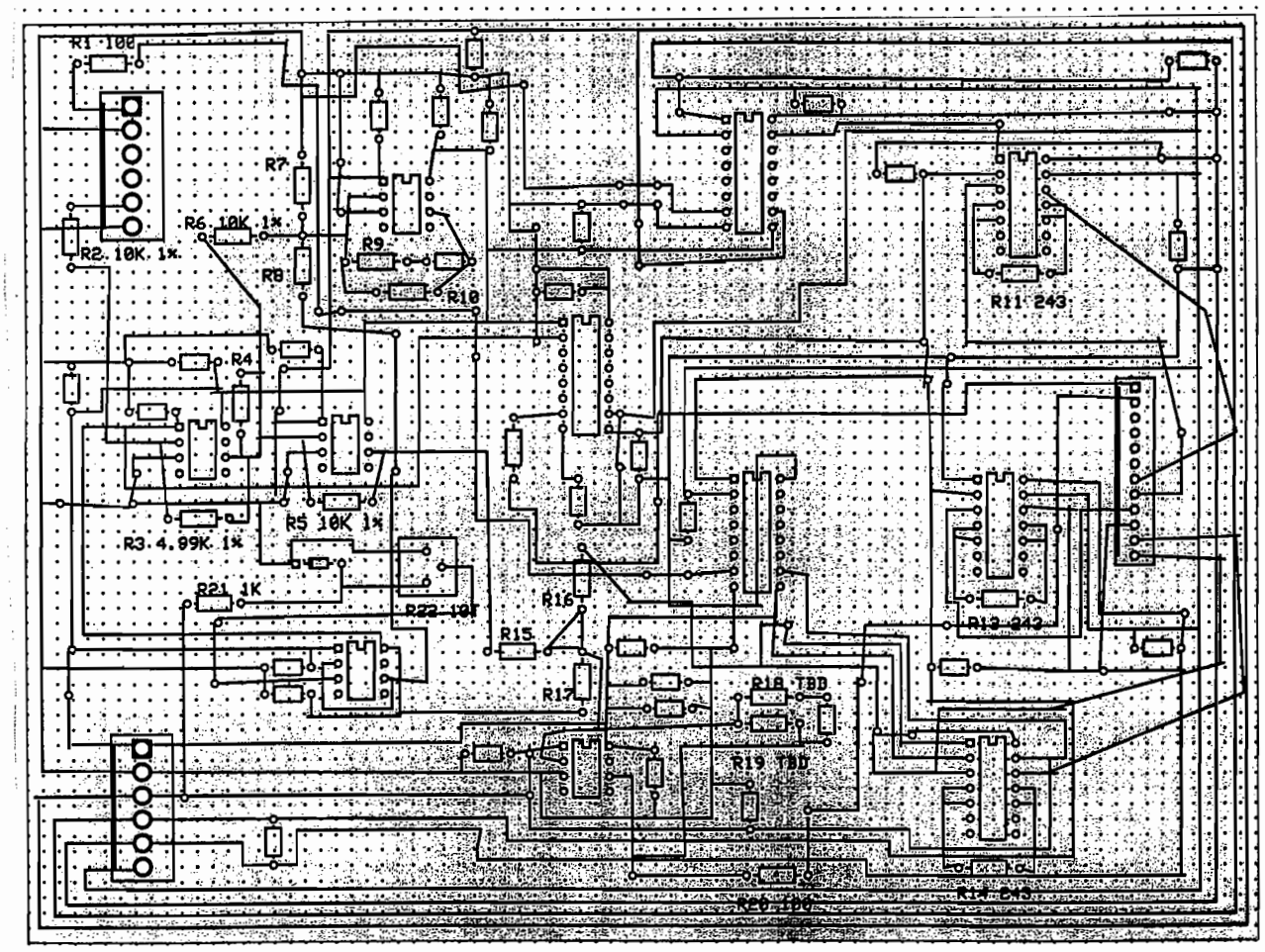

Figure 22: Actual layout of PC Board.

8 Conclusions

Due to space constraints, we resolved to determine whether or not it would be practical to combine two magnets functions into one magnet, how to accomplish that goal, and then finally to build and test the resulting hybrid magnet.

After 10 weeks of work, several of the project goals have been accomplished. First, the initial calculations suggested that indeed a quadrupole could be modified by shunting current from one side to the other to create a dipole field along with the quadrupole field within the newly modified quadrupole. Second, computer simulations using POISSON showed that our initial calculations were close, and that the magnetic deformations caused by this approach were predominently a sextupole moment, with a relative strength of less than 10%, for almost all uses of the steering magnet. Third, we successfully designed and built all the equipment required for this project. This includes not only the passbanks themselves, but also the PC board to control the passbank system, and several interlock systems to protect and further control the entire steering quadrupole assembly. Finally, we rigorously tested the passbanks, looking for signs of instability or inaccuracy. The passbanks performed admirably, passing every test with flying colors, never getting above 68% of the maximum rated temperature, and with current fluctuations within individual MOSFET transistors of less than 1%. Further, all the interlock and safety equipment performed without a hitch, shutting down the entire system before a single component could be damaged over the entire 140 hours of passbank run, excepting a few fuses blown due to initial faulty power supplies, which caused the entire system to shut down just as it should.

A few further analyses of the data could be run in the future. First, the exact strength of the sextupole moment could be calculated, and then compared to known sextupole behavior to predict its effect upon the proton beam. Second, a more exact determination of the maximum current the passbanks can carry could be determined through the rough method of increasing the current until they overload, and observing what effect that has.

In the future, several tests remain to be run. First, the completed quadrupole assembly must be magnetically tested, probably with a hall probe and magnetic field mapper, once again under different configurations, to compare to the simulated results from POISSON. After that the steering